

OVERHUNG ROTOR PASSING TROUGH ITS CRITICAL SPEED

Fredy Coral Alamo

Pontifícia Universidade Católica do Rio de Janeiro – Departamento de Engenharia Mecânica
Rua Marquês de São Vicente, 225 – Gávea, Rio de Janeiro – RJ – Brasil, 22453-900

Hans Ingo Weber

Pontifícia Universidade Católica do Rio de Janeiro – Departamento de Engenharia Mecânica
Rua Marquês de São Vicente, 225 – Gávea, Rio de Janeiro – RJ – Brasil, 22453-900

Abstract. *The purpose of this work is to analyze the overhung rotor dynamics considering the contact phenomenon between the disk and an annular ring. The analysis of contact is particularly complex, due to the high nonlinearity of the motion equations. The impact is accounted by a consistent contact model, the viscoelastic model. Motion equation for the rotor is encountered employing the Lagrangean method. These equations are capable of capturing phenomena due to lateral vibration, like: forward whirl, backward whirl, rolling or sliding along the annular ring. Due to the combined parameters and the effect of nonlinearity in the motion equations, the dynamical response is not simple or easily predictable. Numerical simulation is the preferred method of analysis, here it is used the Runge-Kutta Fehlberg method. Simulation results show that under certain conditions, the rotor changes its orbit due to the impacts with the annular ring and after that, it executes backward whirl motion. It is a kind of phenomenon that is considered as the most violent and dangerous in rotating machines. The passing through its critical speed is analyzed when driven by an electric motor (also when the system operates under a constant rotational velocity).*

Keywords. Rotor Dynamics, Rolling and Sliding, Forward and Backward Whirl, Impact.

1. INTRODUCTION

The study of rotating machines has special importance for industries, due to the huge amount of applications. One of these applications is in oil well drilling, where, the overhung rotor model may represent, satisfactorily, the lateral dynamics of a drill-string section when it is impacting with the wall.

The impact is a complex phenomenon that is still under investigation; a recent work by Schiehlen (2003) shows that the method of multibody systems is most efficient for the dynamical analysis of machines and structures. During impact, kinetic energy is lost by plastic deformations, viscoelastic effects and wave propagation. For rigid body models, like Brach's model (1998), the energy loss is measured macromechanically by the coefficient of restitution. In this work it is used a vibroimpact model, Rajalingham & Rakheja (2000), which represents satisfactorily the impact phenomenon, where the impact force behavior is parabolic.

In order to investigate the dynamics of the system, the equation of motion for the rotor is obtained by the Lagrange approach, and it is solved numerically using the 5th order Runge-Kutta Fehlberg method. Finally, numerical results are compared with those obtained from the related literature.

2. MOTION EQUATIONS

When the rotating disk, Fig. (1A), impacts against the ring, there arise impact forces that act on the disk. In order to calculate these forces, it is used here the vibroimpact model for the normal force and Coulomb's law for the tangential force.

In the mechanical model we have 4DOF: a rigid body rotation of the motor shaft (θ), a torsional deformation (ϕ) of the rotor shaft and two orthogonal lateral deflections of the disk center (x, y). The Lagrange equation for a non-conservative system is:

$$\frac{d}{dt} \left(\frac{\partial T}{\partial \dot{q}_i} \right) - \frac{\partial T}{\partial q_i} + \frac{\partial U}{\partial q_i} + \frac{\partial \mathfrak{R}}{\partial \dot{q}_i} = Q_i ; \quad \frac{\partial \mathfrak{R}}{\partial \dot{q}_i} = \sum_{s=1}^n c_{is} \dot{q}_s \quad (i=1,2,\dots,n) \quad (1)$$

Where T and U are the Kinetic and Potential Energy; \mathfrak{R} is the Rayleigh's energy dissipation function; Q_i are the generalized forces associated with the generalized coordinates

$$q_i = [x \quad y \quad \theta \quad \phi].$$

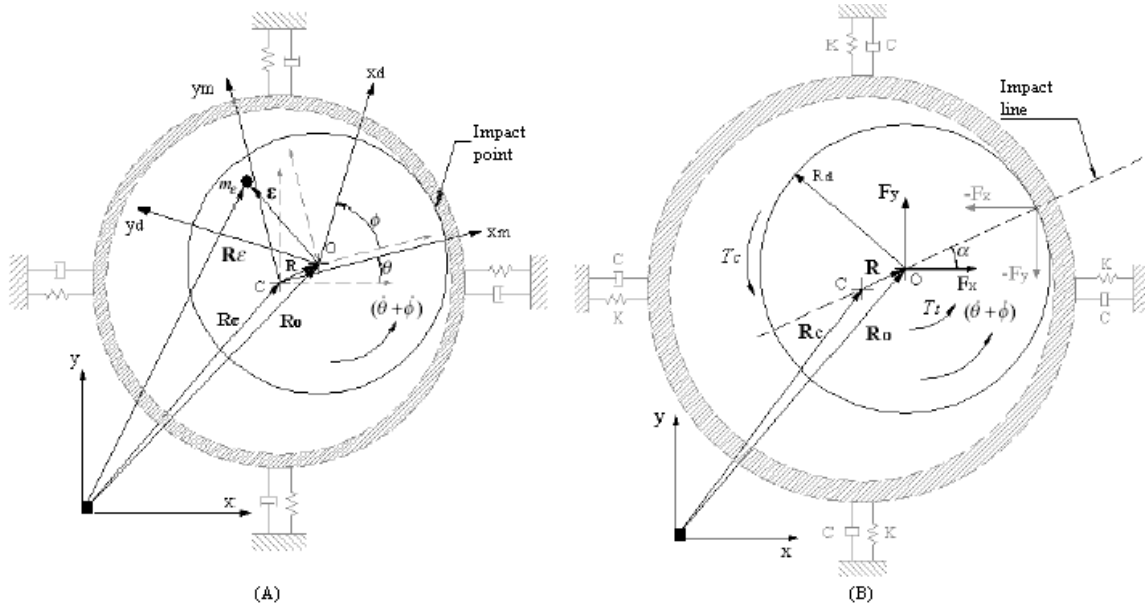


Figure 1. Deformed state of the system (A) and impacting forces on the disk (B)

The expression for the **Kinetic Energy** is:

$$T = \frac{1}{2} m_d (\dot{x}^2 + \dot{y}^2) + \frac{1}{2} J (\dot{\theta} + \dot{\phi})^2 + \frac{1}{2} J_m (\dot{\theta})^2 + \frac{1}{2} m_e (\dot{\mathbf{R}}_e^T \dot{\mathbf{R}}_e)$$

Here, the first term is the translational energy of the disk, the second is the rotational energy of the rotor, the third is the rotational energy of the electric motor shaft, and, the last one is the imbalance energy.

The location of m_e in the inertial system (x, y) is given by: $\mathbf{R}_e = \mathbf{R}_0 + \mathbf{A}(\theta+\phi) \mathbf{\epsilon}$ where: $\mathbf{\epsilon} = [\epsilon_x \quad \epsilon_y]^T$, and $\mathbf{A}(\theta+\phi) = \begin{bmatrix} \cos(\theta+\phi) & -\sin(\theta+\phi) \\ \sin(\theta+\phi) & \cos(\theta+\phi) \end{bmatrix}$ is responsible for the transformation of coordinates $(x, y) \xrightarrow{(\theta+\phi)} (x_d, y_d)$. Finally the derivative of \mathbf{R}_e is define by:

$$\dot{\mathbf{R}}_{\varepsilon} = \dot{\mathbf{R}}_0 + (\dot{\theta} + \dot{\phi}) \begin{bmatrix} -\sin(\theta + \phi) & -\cos(\theta + \phi) \\ \cos(\theta + \phi) & -\sin(\theta + \phi) \end{bmatrix} \mathbf{\varepsilon}$$

Now, writing the Kinetic Energy in the inertial system, results:

$$T = \frac{1}{2} m_d (\dot{x}^2 + \dot{y}^2) + \frac{1}{2} J (\dot{\theta} + \dot{\phi})^2 + \frac{1}{2} J_m (\dot{\theta})^2 + \frac{1}{2} m_{\varepsilon} [(\dot{\theta} + \dot{\phi})(-\varepsilon_x \sin(\theta + \phi) - \varepsilon_y \cos(\theta + \phi)) + \dot{x}]^2 + \frac{1}{2} m_{\varepsilon} [(\dot{\theta} + \dot{\phi})(-\varepsilon_y \sin(\theta + \phi) + \varepsilon_x \cos(\theta + \phi)) + \dot{y}]^2$$

The expression for the **Potential Energy** is:

$$U = \frac{1}{2} k_b x^2 + \frac{1}{2} k_b y^2 + \frac{1}{2} k_t \phi^2$$

Here, the first and second terms are the energy due to shaft flexion and the last one is due to shaft torsion.

The expressions for the **Rayleigh's Energy Dissipation Function**, considering viscous damping, proportional and non coupled, are:

$$\frac{\partial \mathfrak{R}}{\partial \dot{x}} = c_{xx} \dot{x}, \quad \frac{\partial \mathfrak{R}}{\partial \dot{y}} = c_{yy} \dot{y}, \quad \frac{\partial \mathfrak{R}}{\partial \theta} = 0 \quad \text{e} \quad \frac{\partial \mathfrak{R}}{\partial \dot{\phi}} = c_{\phi\phi} \dot{\phi}$$

Where, $c_{xx} = c_{yy} = c_b$ and $c_{\phi\phi} = c_t$ are the flexural and torsional damping coefficients, respectively.

Considering that the vector of generalized forces, for 4DOF, is given by: $\mathbf{Q} = [Q_x \ Q_y \ Q_{\theta} \ Q_{\phi}]^T$, and, using the Lagrange equation, Eq. (1), results four equations for the variables (x, y, θ, ϕ) .

The motion equation, in matrix form $\mathbf{M} \ddot{\mathbf{Z}} + \mathbf{C} \dot{\mathbf{Z}} + \mathbf{K} \mathbf{Z} + \mathbf{P} = \mathbf{Q}$, results:

$$\begin{bmatrix} m_1 & 0 & m_2 & m_2 \\ 0 & m_1 & m_3 & m_3 \\ m_2 & m_3 & m_4 & m_5 \\ m_2 & m_3 & m_5 & m_5 \end{bmatrix} \begin{bmatrix} \ddot{x} \\ \ddot{y} \\ \ddot{\theta} \\ \ddot{\phi} \end{bmatrix} + \begin{bmatrix} c_b & 0 & 0 & 0 \\ 0 & c_b & 0 & 0 \\ 0 & 0 & 0 & 0 \\ 0 & 0 & 0 & c_t \end{bmatrix} \begin{bmatrix} \dot{x} \\ \dot{y} \\ \dot{\theta} \\ \dot{\phi} \end{bmatrix} + \begin{bmatrix} k_b & 0 & 0 & 0 \\ 0 & k_b & 0 & 0 \\ 0 & 0 & 0 & 0 \\ 0 & 0 & 0 & k_t \end{bmatrix} \begin{bmatrix} x \\ y \\ \theta \\ \phi \end{bmatrix} = \begin{bmatrix} P_x \\ P_y \\ Q_{\theta} \\ Q_{\phi} \end{bmatrix} \quad (2)$$

The mass matrix elements are:

$$m_1 = m_d + m_{\varepsilon}; \quad m_2 = -m_{\varepsilon} [\varepsilon_x \sin(\theta + \phi) + \varepsilon_y \cos(\theta + \phi)]; \\ m_3 = +m_{\varepsilon} [\varepsilon_x \cos(\theta + \phi) - \varepsilon_y \sin(\theta + \phi)]; \quad m_4 = m_{\varepsilon} \varepsilon^2 + J + J_m; \quad m_5 = m_{\varepsilon} \varepsilon^2 + J$$

The non-linear forces, which represent the centrifugal forces, are:

$$P_x = -m_{\varepsilon} (\dot{\theta} + \dot{\phi})^2 [\varepsilon_x \cos(\theta + \phi) - \varepsilon_y \sin(\theta + \phi)]$$

$$P_y = -m_{\varepsilon} (\dot{\theta} + \dot{\phi})^2 [\varepsilon_x \sin(\theta + \phi) + \varepsilon_y \cos(\theta + \phi)]$$

In Eq. (2), the determinant of the mass matrix $|\mathbf{M}| = J_m(m_d + m_{\varepsilon})(m_d J + m_d m_{\varepsilon} \varepsilon^2 + m_{\varepsilon} J)$ is a number, then, we will not have any singularity problems when the motion equation is solved numerically.

The impacting forces, Fig. (1B), in the inertial system (x, y) can be calculated as:

$$F_n = \left\{ K_c (R - \delta) + C_c \frac{d}{dt} (R - \delta) \right\} H_{(R-\delta)}; \quad F_t = \mu F_n; \quad R = \sqrt{(x - X)^2 + (y - Y)^2};$$

Where K_c is the contact stiffness; C_c is the contact damping coefficient; δ is the radial gap and $H_{(R-\delta)}$ is the Heavyside function. The impact force components and torque in the coordinate system (x, y) result:

$$\begin{bmatrix} F_x \\ F_y \end{bmatrix} = \left(\frac{F_n}{R} \right) \begin{bmatrix} +(y - Y) & -(x - X) \\ -(x - X) & -(y - Y) \end{bmatrix} \begin{bmatrix} \mu \\ 1 \end{bmatrix}; \quad T_t = -F_t R_d$$

Finally, the generalized forces \mathbf{Q} corresponding to the external forces, acting on the disk, are

$$\mathbf{Q} = [Q_x \quad Q_y \quad Q_{\theta} \quad Q_{\phi}]^T = [F_x \quad F_y \quad T_m \quad T_t]^T$$

Where T_m is the torque acting on the rotor: it was found from experiments that is a polynomial function ($C = \frac{150}{66}$ is a constant and Ω rad/s is the rotor's rotational speed)

$$T_m = C \left[-0.002441 \left(\frac{\Omega}{C} \right)^3 + 0.177 \left(\frac{\Omega}{C} \right)^2 - 5.608 \left(\frac{\Omega}{C} \right) + 290.65 \right] \text{N-mm}$$

3. NUMERICAL EXAMPLE

For the numerical simulations the initial disk center position coincides with the shaft motor center, and, the disk velocity is zero (zero initial condition). Table (1) show us numerical values, some of them were obtained from an experimental test rig, and, other from the literature review.

For this simulation, the disk behavior is analyzed in two cases: without and with the annular ring of the rotor system. The results without the ring are showed in Fig. (2): it is a typical dynamical system behavior passing through its critical speed ($\omega_c = 2.29$ Hz.). Firstly the disk orbit starts at the point (0,0) and due to the motor torque; the disk orbit grows, after reaching the maximum orbit amplitude ≈ 7 mm. (near its critical speed), the disk orbit decreases until it reaches the steady-state motion. Fig. (2) shows clearly that the frequency where there occurs the maximum orbit amplitude is moving to the right side of the critical speed, when the torque is increasing. The new frequencies for the maximum orbit are $1.16(\omega_c)$, $1.53(\omega_c)$ and $3.10(\omega_c)$ Hz for the 1%, 10% and 100% T_m , respectively. Childs (1993) and Markert & Seidler (2001) also name this behavior.

Table 1. Geometrical and physical parameters for the rotor dynamic system

Disk		
Mass (kg), radius (mm)	m_d, R_d	2.5, 50
Annular Ring		
Inner radius (mm)	R_e	50.9
Shaft		
Flexural stiffness (N/m)	K_b	506.1
Torsional stiffness (N-m/rad)	K_t	51.8
Torsional and Flexural damping factor	ζ_t, ζ_b	0.01
Contact parameters		
Contact stiffness (N/m)	K_c	1.0×10^6
Viscous coefficient of proportionality (s)	β	1.0×10^{-7}
Contact damping coefficient (N-s/m)	$C_c = \beta K_c$	0.1
Eccentricity		
Mass (kg)	m_e	0.03
Coordinates $(\varepsilon_x, \varepsilon_y)$ (mm)	$\varepsilon_x, \varepsilon_y$	28.2, 28.2

Here it is necessary to point out that when there is low damping in the system, Eq. (1), the transient don't dies away in the resonance curve and the solution of the system looks like the Fig. (2). Now, let us consider the annular ring in the rotor system and apply a 100% T_m . In this case, the radial gap between the annular ring and the disk is considered 0.9 mm; therefore, it is expected that the disk impact the ring, since it will restrict its free motion. Fig. (3) shows us the disk orbit and resonance curve for two different values of the friction coefficient μ (0.01 and 0.2). There, we can see that for a low friction coefficient ($\mu = 0.01$), the disk, after some impacts, is moving in a forward whirl form Fig. (3A), on the other hand, when the friction coefficient is high ($\mu = 0.2$) the backward whirl motion is occurring Fig. (3C). Bartha (2001), who observed a strong dependence of the friction coefficient to induce the whirl phenomena in the disk, also pointed out this same behavior.

4. CONCLUSIONS

The study of the rotating system includes the free passing through its critical speed and the motion when an annular ring limits the disk. When it is passing its critical speed, we found out that the frequency where the maximum orbit amplitude occurs is varying with the torque on the rotor. For higher torques the new frequencies moves to the right side of the critical speed. Also, it is necessary to point out that when there is low damping in the system, as used for the numerical simulation, the transient don't dies away in the resonance curves and the solution of the system looks like the obtained curve.

This work shows that there is a strong dependence of the friction coefficient to induce the whirl movement. For low friction coefficient, the disk develops forward whirl, and, backward whirl when the friction coefficient is high. In the process of validation of the developed model, one interesting conclusion is that the backward whirl can be avoided decreasing the amount of friction present at the surfaces that get in contact.

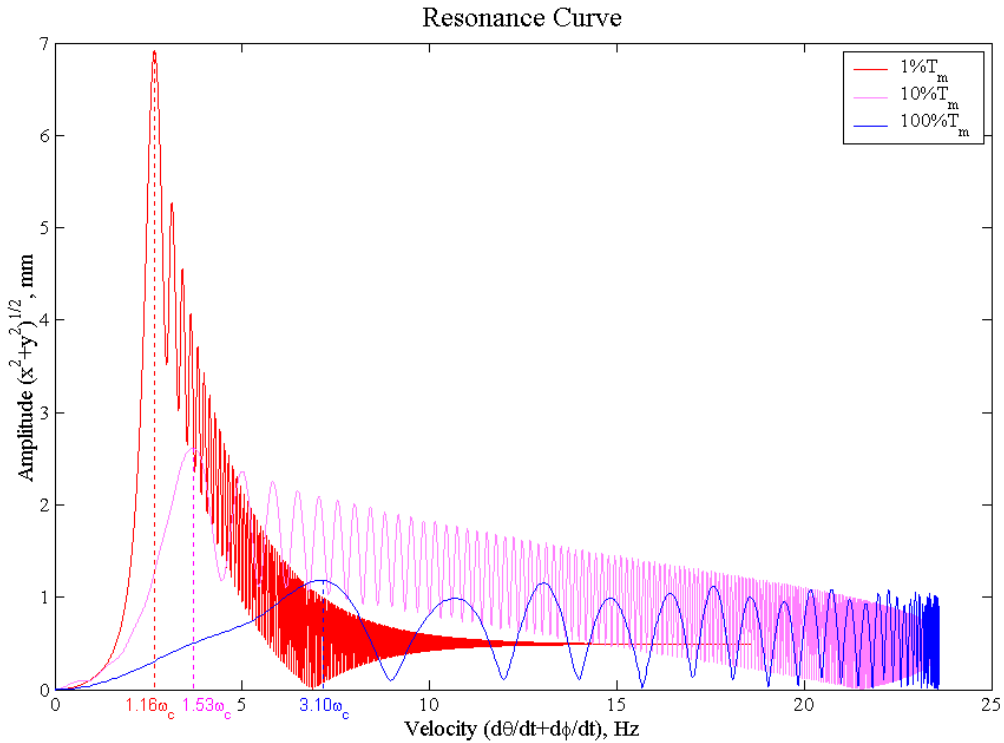


Figure 2. Resonance curve for various motor torques without annular ring

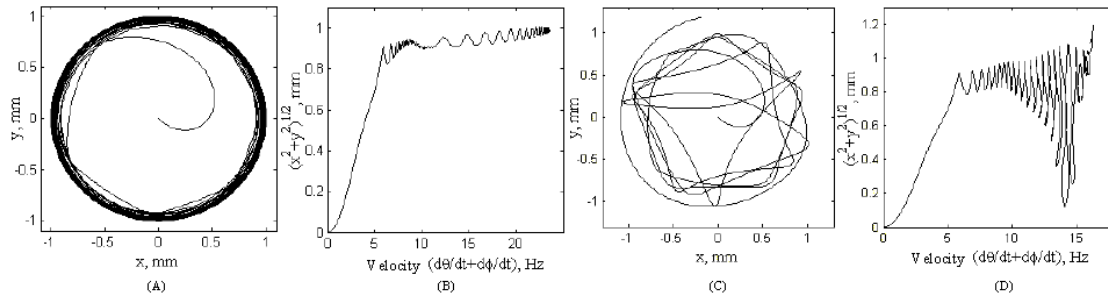


Figure 3. Disk's orbit and resonance curve (A, B for $\mu = 0.01$ and C, D for $\mu = 0.2$)

5. REFERENCES

Coral, F., 2003, “Dinâmica de um rotor vertical em balanço com impacto”, Dissertação, PUC-Rio.

Schiehlen, W. and Seifried, R., 2003, “Impact Models: From Wave Propagation to Body Motion”, X DINAME, Ubatuba, SP -Brazil, pg. 77-81.

Coral, F. and Weber, H. I., 2003, “Mathematical model for a rotating overhung rotor”, XXIV Iberian Latin-American Congress on Computational Methods in Engineering, XXIV CILAMCE, Ouro Preto (Brazil), October 2003.

Bartha, A. R., 2001, “Dry Friction Backward Whirl of Rotors”, Diss., Technische Wissenschaften.

Markert, R. and Seidler, M., 2001, “Analytically Based Estimation of the Maximum Amplitude During Passage Through Resonance”, Int. Journal of Solids and Structures, Vol. 38, Issue 10-13.

Brach, R. M., 1998, “Formulation of Rigid Body Impact Problems Using Generalized Coefficients”, Int. J. Engng Sci. Vol. 36, No. 1, pp. 61-71.

Childs, D., 1993, “Turbomachinery Rotordynamics”, John Wiley & Sons.